J. Phys. D: Appl. Phys. **42** (2009) 015305 (4pp) doi:10.1088/0022-3727/42/1/015305

# Self-assembled Sn nanoplatelets on Si(1 1 1)-$2\sqrt{3} \times 2\sqrt{3}$-Sn surfaces

**Quantong Shen[1], Wenjuan Li[1], Guocai Dong[1], Guofeng Sun[1], Yujie Sun[2], Xucun Ma[1], Jinfeng Jia[2] and Qikun Xue[1,2]**

[1] Institute of Physics, Chinese Academy of Sciences, Beijing 100190, People's Republic of China
[2] Department of Physics, Tsinghua University, Beijing 100084, People's Republic of China

Received 30 July 2008, in final form 11 October 2008
Published 10 December 2008
Online at stacks.iop.org/JPhysD/42/015305

**Abstract**
Room temperature growth of Sn on Sn-induced Si(1 1 1)-$2\sqrt{3} \times 2\sqrt{3}$ surfaces is investigated by scanning tunneling microscopy. On the Si(1 1 1)-$2\sqrt{3} \times 2\sqrt{3}$-Sn surfaces, uniform arrays of hexagonal Sn nanoplatelets with narrow lateral size distribution are obtained. The experimental data show that the preferred lateral island size varies with Sn coverage. This variation can be explained in terms of island–island interactions. As a result of quantum size effects, the Sn islands exhibit preferred heights.

(Some figures in this article are in colour only in the electronic version)

## 1. Introduction

Self-assembled nanoparticles (or islands) with narrow size distribution have great potential in optical, electronic and magnetic device applications. The strain energy originated from the lattice mismatch between islands and substrate has been exploited to produce self-assembled islands. Semiconductor quantum dots with uniform sizes were obtained in Ge/Si(0 0 1) and InGaAs/GaAs(0 0 1) systems [1–3]. In these cases, three-dimensional (3D) islands spontaneously form on a wetting layer on a substrate via Stranski–Krastanow mode, in contrast to Volmer–Weber mode where 3D islands nucleate directly on a substrate. Theories are proposed to explain the size selection of islands. Some attribute it to strain-induced equilibrium states while others propose that the island edge effect induces a stable island size against ripening [4, 5]. Besides the factors external to growing islands, it has also been shown that the size selection of islands could be achieved via the forces confined to the interiors of the islands [6]. For metals, the size distribution of 3D metal islands is broad in general [7–10] in spite of some reports on uniform 3D metal islands such as Au on $TiO_2$ surface and Fe on the NaCl(0 0 1) surface [11, 12]. The physical origin underlying the size selection is not yet fully understood.

In this work, we investigate the growth of Sn islands on Sn-induced Si(1 1 1)-$2\sqrt{3} \times 2\sqrt{3}$ by scanning tunnelling microscopy (STM). Sn has two allotropic forms: grey Sn is a semiconducting phase with a diamond structure ($\alpha$-Sn, lattice constant = 6.485 Å), stable at a temperature below 13.2 °C, while white Sn is a metallic phase with a body-centred-tetragonal (BCT) structure ($\beta$–Sn, lattice constant $a = b =$ 5.831 Å, $c = 3.182$ Å), stable for $T > 13.2$ °C. Growth of Sn thin films on the Si(1 1 1) surface has been investigated previously. At room temperature, Sn grows epitaxially with the BCT structure on both Si(1 1 1)-7 × 7 and Si(1 1 1)-$2\sqrt{3} \times 2\sqrt{3}$-Sn surfaces [13]. As the coverage increases, there is a structure transition from unstable $\alpha$-like Sn to $\beta$-Sn islands [14]. We also used the Si(1 1 1)-7 × 7 substrate for both room temperature and low temperature (140 K) growth of Sn. At room temperature, Sn does not form a regular Sn island array at low coverage, whereas at low temperature (140 K) a regular island array forms at 3 ML. If the coverage is increased to 6 ML, Sn islands merge to larger flat-top islands, which cross several substrate terraces. We show that, by optimizing the deposition conditions, a uniform array of narrow sized Sn nanoplatelets could be obtained on Si(1 1 1)-$2\sqrt{3} \times 2\sqrt{3}$-Sn surfaces. Furthermore, the lateral and vertical sizes of the islands in the array could be tuned by the Sn coverage. The self-assembled and size-controlled nanoplatelets provide a unique system for studying superconductivity at reduced dimensionality.

## 2. Experimental details

All experiments were performed on an OMICRON ultra-high vacuum STM system combined with molecular beam

 

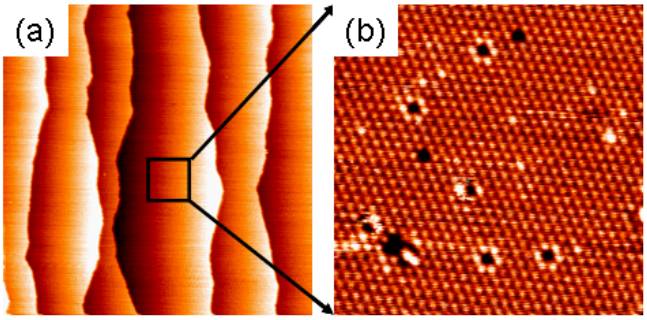


**Figure 1.** STM images of the Si(1 1 1)-$2\sqrt{3} \times 2\sqrt{3}$-Sn reconstruction surface: (*a*) the large-scale scan image 500 nm × 500 nm, (*b*) the zoom-in image 15 nm × 15 nm, its sample bias voltages +2.0 V.

epitaxy. The base pressure of the system is better than $1 \times 10^{-10}$ Torr. The substrates were p-type Si(1 1 1) wafers with the resistivity of 9–11 Ω cm. The standard degassing and flashing procedures were used to obtain clean Si(1 1 1)-7 × 7 surfaces [15]. The Si(1 1 1)-$2\sqrt{3}\times2\sqrt{3}$-Sn reconstruction was prepared by depositing more than 1.3 ML Sn onto the Si(1 1 1)-7 × 7 surface at 400 °C [16]. At room temperature, a very sharp $2\sqrt{3} \times 2\sqrt{3}$ reflection high-energy electron diffraction pattern can be observed from the surface. Figure 1(*a*) shows the morphology of the Si(1 1 1)-$2\sqrt{3} \times 2\sqrt{3}$-Sn surface. The surface is characterized with a well-defined terrace-plus-step structure with a terrace width of about 100 nm. Figure 1(*b*) shows that the $2\sqrt{3} \times 2\sqrt{3}$-Sn reconstruction and vacancy defects can be observed on the surface.

The deposition of Sn on Si(1 1 1)-$2\sqrt{3}\times2\sqrt{3}$-Sn surfaces was performed at room temperature. Sn was evaporated from a pyrolytic boron nitride (PBN) crucible with flux rates ranging from 0.13 to 2.0 ML min$^{-1}$.

All STM topographic images were taken at room temperature with a tunnelling current of 20 pA and a sample bias of 3.0 V. We did not observe a significant difference in the morphology of the Sn islands at different sample voltages.

## 3. Results and discussion

Shown in figure 2 are the STM images of Sn islands grown on Si(1 1 1)-$2\sqrt{3}\times2\sqrt{3}$-Sn surfaces at room temperature for three different coverages. The deposition rate was 2.0 ML min$^{-1}$. Islands with different diameters appear randomly over the surface at the 0.5 ML, as shown in figure 2(*a*). When the Sn coverage increases to 1.0 ML, the islands grow larger and taller. Meanwhile, the islands density drops rapidly. The number of small islands at 1.0 ML is much lesser than that at 0.5 ML. At 2.0 ML, there are only large and high Sn islands on the surface. The decrease in island density with increasing coverage indicates that Sn island growth is in the ripening regime; big Sn islands grow at the expense of small islands nearby. At both 0.5 and 1.0 ML, the large islands are hexagonal and all islands become hexagonal at 2.0 ML.

Figures 2(*d*)–(*f*) show the coverage dependence of the island lateral size. An interesting observation is that, with increasing coverage, there exists a preferred lateral size in the islands at 1.0 and 2.0 ML (see figures 2(*e*) and (*f*)). For 1.0 ML, the centre and the dispersion of a Gaussian fit of the diameter distribution is 10.0 nm and 2.3 nm, respectively, if only the main (right) fitting peak is considered in figure 2(*e*). At 2.0 ML, the two values change to 14.7 nm and 4.2 nm, respectively (figure 2(*f*)). With increasing coverage, the lateral size distribution is broadened much, as is expected in the ripening regime [17]. It was shown that the island edge effect arising from intrinsic surface stress of the islands and substrate induces a stable island size against coarsening and facilitates the island size uniformity [5]. Contribution of the edge effect to the elastic relaxation has a minimum in energy as a function of the island size. Thus the preferred lateral sizes of Sn islands at different coverages indicate that the chemical potential of the Sn island arrays has an energy minimum at the observed lateral size for a given coverage. Furthermore, the preferred lateral size of Sn islands varies as the coverage increases, implying that island–island interactions contribute substantially to the chemical potential of islands [12].

In contrast to the island size change, their shape remains hexagonal as they grow. The island shape can be imposed by the underlying surface reconstruction. On the Si(0 0 1)-c(4 × 12)-Al reconstruction [18], In islands form with an elongated hut shape at different coverages due to the anisotropy diffusion of In atoms. The hexagonal islands come from the isotropic structure nature of the Si(1 1 1)-$2\sqrt{3} \times 2\sqrt{3}$-Sn surface.

Another striking observation is that the diameter distributions of Sn islands shown in figures 2(*d*) and (*e*) are bimodal, which is not in agreement with the standard model of coarsening that invariably gives a unimodal size distribution [17]. At the low coverage of 0.5 ML (figure 2(*d*)), the diameter distribution cannot be fitted by one Gaussian curve. There is a shoulder at the right side of the main peak. At 1.0 ML, the bimodal distribution is more obvious (figure 2(*e*)). The Gaussian fit has two peaks at 4.8 nm and 10.0 nm with a dispersion of 1.7 nm and 2.3 nm, respectively. The distribution returns to the normal unimodal one at the coverage of 2.0 ML.

The influence of deposition rate on the island density and size was also studied. The STM images shown in figures 3(*a*)–(*d*) are the results at deposition rate of 2.0 ML min$^{-1}$, 1.0 ML min$^{-1}$, 0.33 ML min$^{-1}$ and 0.13 ML min$^{-1}$, respectively. The corresponding histograms of diameter distributions are shown in figures 3(*e*)–(*h*). The total surface coverage is 1.0 ML. The island density varies little with the increasing deposition rate, and the diameter distributions are essentially bimodal.

Bimodal distribution was observed in the Ge/Si(0 0 1) system where two kinds of Ge islands with distinct shapes coexist on the Si(0 0 1) surface under certain growth conditions [19]. The metallic islands are different from semiconductor islands in that the former can change their shape continuously, while the latter does not, which can jump from one to another. The appearance of two different diameters of the Sn islands indicates that the peaks correspond to metastable states. The first peak is due to probably the lateral quantum size effects, in which the motions of electrons in Sn islands are confined in the two-dimensional planes perpendicular to Sn islands and

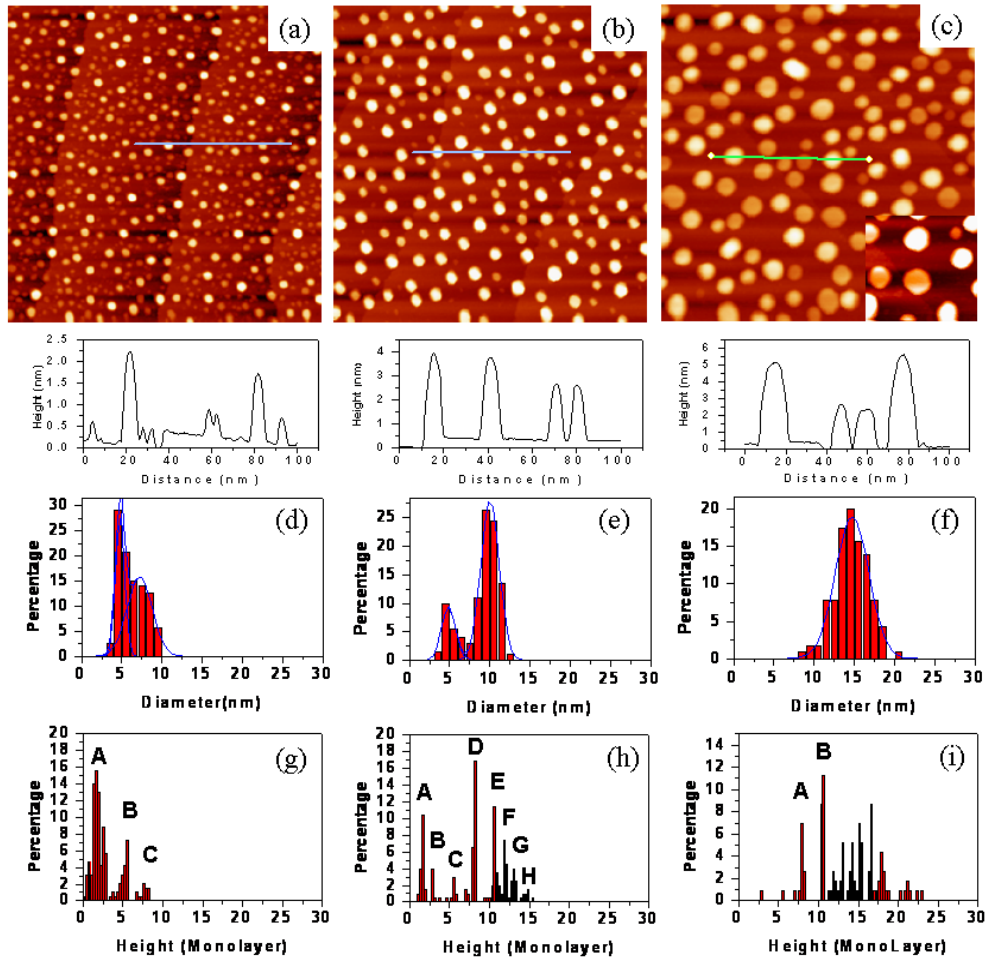


**Figure 2.** STM images (the upper panel, (*a*)–(*c*)), corresponding diameter (the middle panel, (*d*)–(*f*)) and height (the bottom panel, (*g*)–(*i*)) histograms of Sn islands grown on Si(1 1 1)-2$\sqrt{3}$ × 2$\sqrt{3}$-Sn surfaces at three different coverages (0.5, 1.0 and 2.0 ML). The surface coverage is (*a*) 0.5 ML, (*b*) 1.0 ML and (*c*) 2.0 ML. The image sizes are all 200 nm × 200 nm. The inset of figure 2(*c*) is a zoom-in STM image of Sn islands. The cross-section height profile obtained from the line marked in the STM image is also shown right below the STM image. The interlayer spacing *d* along the [0 0 1] direction of metallic Sn with BCT structure is chosen as the unit of Sn island heights in (*g*)–(*i*).

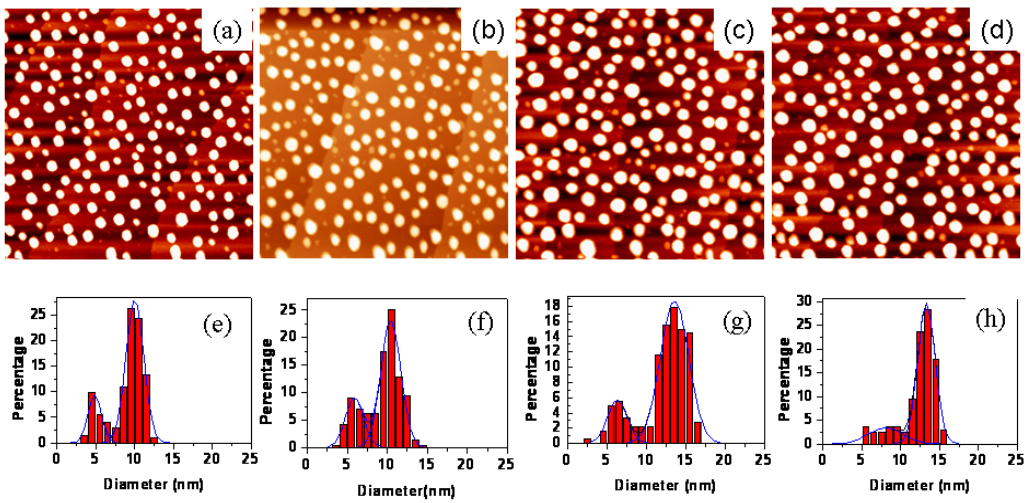


**Figure 3.** STM images (the upper panel) and corresponding diameter histograms (the lower panel) of Sn islands grown on Si(1 1 1)-2$\sqrt{3}$ × 2$\sqrt{3}$-Sn surfaces for a surface coverage of 1.0 ML at different deposition rates: (*a*) and (*e*) 2.0 ML min$^{-1}$, (*b*) and (*f*) 1.0 ML min$^{-1}$, (*c*) and (*g*) 0.33 ML min$^{-1}$, (*d*) and (*h*) 0.13 ML min$^{-1}$. The image sizes are all 200 nm × 200 nm.

standing waves are formed. The second and main peak is from the island edge effect. These preferential island sizes are mainly related to the coverage through the island density, which does not change much with the deposition rate in this experiment.

The height distribution as a function of coverage is shown in figures 2(*g*)–(*i*). The island heights were measured from the top of the wetting layer. Due to the finite size of STM tips and the fact that Sn islands are tall, the apparent island heights are larger than the actual values. At the low coverage of 0.5 ML (figure 2(*a*)), a significant fraction of small islands one or two atomic-layer high is observed, corresponding to peak A in figure 2(*g*). The taller islands have a height of five or seven monolayers, corresponding to peaks B and C in figure 2(*g*), respectively. Assuming that the vertical layer spacing in the Sn islands is close to the corresponding value in metallic bulk Sn with BCT structure, the double-layer increment in the Sn island height is obvious. At 1.0 ML, the preferred heights of big islands are five, seven and nine atomic layers (peaks C, D and E in figure 2(*h*)), and seven layers appear most frequently. The phenomenon is quite robust and remains at higher coverage (see peaks A and B in figure 2(*i*) for the coverage of 2 ML).

The unusual growth mode of preferential island or film heights has been observed in Ag/GaAs and Pb/Si(1 1 1) systems [20] and was attributed to quantum size effects due to the vertical confinement of electron motion [21]. For metallic Sn with BCT structure, the interlayer spacing $d$ along the [0 0 1] direction is one-half of the lattice constant, $d = a/2 = 0.29$ nm. The Fermi wavelength along this direction is $\lambda_F = 0.388$ nm. It leads to a relation $d \approx 3\lambda_F/4$. The relation means that three nodes of electron waves are exactly introduced for a change in two-atomic-layers. Islands with a height integer times of $3\lambda_F/2$ are favoured by quantum size effects. The existence of quantum well states in Sn islands grown on Si(1 1 1)-$2\sqrt{3} \times 2\sqrt{3}$-Sn surfaces was confirmed by scanning tunnelling spectroscopy [22]. With increasing height, the quantum size effects become weak and islands will change height continuously at a certain point. This was indeed observed (see peaks F, G and H in figure 2(*h*)), when the height is greater than nine atomic layers.

## 4. Summary

Sn island arrays with uniform lateral sizes were obtained on Si(1 1 1)-$2\sqrt{3} \times 2\sqrt{3}$-Sn surfaces. The narrow lateral size distribution in Sn islands is shown to be a result of the island edge effect. The observed coverage dependent preferred lateral sizes suggest that the island–island interactions play the main role in the self-assembly of Sn islands.

## Acknowledgment

This work was supported by National Science Foundation and Ministry of Science and Technology of China.

## References

[1] Shchukin V A and Bimberg D 1999 *Rev. Mod. Phys.* **71** 1125
[2] Mo Y-W, Savage D E, Swartzentruber B S and Lagally M G 1990 *Phys. Rev. Lett.* **65** 1020
[3] Leonard D, Krishnamurthy M, Reaves C M, Denbaars S P and Petroff P M 1993 *Appl. Phys. Lett.* **63** 3203
[4] István D and Alert-László B 1997 *Phys. Rev. Lett.* **79** 3708
[5] Shchukin V A, Ledentsov N N, Kop'ev P S and Binberg D 1995 *Phys. Rev. Lett.* **75** 2968
Liu F 2002 *Phys. Rev. Lett.* **89** 246105
[6] Tokar V I and Dreyssé H 2005 *Phys. Rev.* B **72** 035438
[7] Sugawara A and Scheinfein M R 1997 *Phys. Rev.* B **56** R8499
[8] Huang L, Chey S J and Weaver J H 1998 *Phys. Rev. Lett.* **80** 4095
[9] Fruchart O, Klaua M, Barthel J and Kirschner J 1999 *Phys. Rev. Lett.* **83** 2769
[10] Yu C T, Li D Q, J. Pearson J and Bader S D 2001 *Appl. Phys. Lett.* **79** 3848
[11] Xu C, Lai X and Goodman D W 1997 *Phys. Rev.* B **56** 13464
[12] Gai Z, Wu B, Pierce J P, Farnan G A, Shu D, Wang M, Zhang Z and Shen J 2002 *Phys. Rev. Lett.* **89** 235502
[13] Ryu J T, Katayama M and Oura K 2002 *Surf. Sci.* **515** 199
[14] Wang D T, Esser N, Cardona M and Zegenhagen J 1995 *Surf. Sci.* **343** 31
[15] Li J-L, Jia J-F, Liang X-J, Liu X, Wang J-W, Xue Q-K, Li Z Q, Tse J S, Zhang Z Y and Zhang S B 2002 *Phys. Rev. Lett.* **88** 066101
[16] Ichikawa T 1984 *Surf. Sci.* **140** 37
[17] Zinke-Allmang M, Felman L C and Grabow M H 1992 *Surf. Sci. Rep.* **16** 377–463
[18] Gruznev D V, Olyanich D A, Avilov V A, Saranin A A and Zotov A V 2006 *Surf. Sci.* **600** 4986
[19] Tomitori M, Watanabe K, Kobayashi M and Nishikawa O 1994 *Appl. Surf. Surf.* **76/77** 322
[20] Smith A R, Chao K-J, Niu Q and Shih C-K 1996 *Science* **273** 226
Su W B, Chang S H, Jian W B, Chang C S, Chen L J and Tsong T T 2001 *Phys. Rev. Lett.* **86** 5116
[21] Zhang Z, Niu Q and Shih C-K 1998 *Phys. Rev. Lett.* **80** 5381
[22] Wang L L, Ma X C, Ji S H, Fu Y S, Shen Q T, Jia J F, Kelly K F and Xue Q K 2008 *Phys. Rev.* B **77** 205410